Brain Stimulation 15 (2022) 391–402

Contents lists available at ScienceDirect

Brain Stimulation

journal homepage: http://www.journals.elsevier.com/brain-stimulation

# Prefrontal theta phase-dependent rTMS-induced plasticity of cortical and behavioral responses in human cortex

Pedro Caldana Gordon [a, b], Paolo Belardinelli [a, b, c], Matti Stenroos [d], Ulf Ziemann [a, b, *], Christoph Zrenner [a, b, e]

[a] Department of Neurology & Stroke, University of Tübingen, Germany
[b] Hertie Institute for Clinical Brain Research, University of Tübingen, Germany
[c] CIMeC, Center for Mind/Brain Sciences, University of Trento, Italy
[d] Department of Neuroscience and Biomedical Engineering, Aalto University School of Science, Espoo, Finland
[e] Temerty Centre for Therapeutic Brain Intervention, Centre for Addiction and Mental Health, and Department of Psychiatry, University of Toronto, Toronto, ON, Canada

ARTICLE INFO

*Article history:*
Received 29 September 2021
Received in revised form
4 January 2022
Accepted 14 February 2022
Available online 17 February 2022

*Keywords:*
EEG-TMS
Prefrontal cortex
Brain-state-dependent stimulation
Theta oscillation
Phase-amplitude coupling
Working memory

ABSTRACT

*Background:* Prefrontal theta oscillations are involved in neuronal information transfer and retention. Phases along the theta cycle represent varied excitability states, whereby high-excitability states correspond to high-frequency neuronal activity and heightened capacity for plasticity induction, as demonstrated in animal studies. Human studies corroborate this model and suggest a core role of prefrontal theta activity in working memory (WM).

Objective/Hypothesis: We aimed at modulating prefrontal neuronal excitability and WM performance in healthy humans, using real-time EEG analysis for triggering repetitive transcranial magnetic stimulation (rTMS) theta-phase synchronized to the left dorsomedial prefrontal cortex.

*Methods:* 16 subjects underwent 3 different rTMS interventions on separate days, with pulses triggered according to the individual's real-time EEG activity: 400 rTMS gamma-frequency (100 Hz) triplet bursts applied during either the negative peak of the prefrontal theta oscillation, the positive peak, or at random phase. Changes in cortical excitability were assessed with EEG responses following single-pulse TMS, and behavioral effects by using a WM task.

*Results:* Negative-peak rTMS increased single-pulse TMS-induced prefrontal theta power and theta-gamma phase-amplitude coupling, and decreased WM response time. In contrast, positive-peak rTMS decreased prefrontal theta power, while no changes were observed after random-phase rTMS.

*Conclusion:* Findings point to the feasibility of EEG-TMS technology in a theta–gamma phase–amplitude coupling mode for effectively modifying WM networks in human prefrontal cortex, with potential for therapeutic applications.



## 1. Introduction

Brain oscillations mediate information flow and storage in neuronal networks [1]. Oscillatory activity in the theta band (4–8 Hz) is of particular interest, as it has been associated with several cognitive processes in both animal models and human subjects [2–4]. It has been proposed that neuronal theta-band activity produces alternation of excitation and inhibition states, in accordance to the phases of the oscillation, enabling distant neuronal populations to exchange information when their activity is timely coupled, and to disregard non-coupled, potentially irrelevant information [5]. Several studies with behaving human subjects have observed an increase in theta oscillatory power during the execution of cognitive tasks [6–8]. Furthermore, high-frequency neuronal activity (in the gamma-frequency band, >30 Hz) and neuronal spiking were observed to occur preferentially in specific phases of the theta oscillation in prefrontal cortex and hippocampus. These observations suggest that different phases of low-frequency rhythms define local states of neuronal excitability, that is the current propensity of a neuronal population to discharge

* Corresponding author. Department of Neurology & Stroke, University of Tübingen, Germany.
*E-mail address:* ulf.ziemann@uni-tuebingen.de (U. Ziemann).

https://doi.org/10.1016/j.brs.2022.02.006

action potentials in response to incoming stimuli and, therefore, transmit downstream information. It follows that, in a neuronal population operating in synchrony with that low-frequency oscillation, stimuli arriving during the high-excitability phase of that oscillation would lead to an effective neuronal response and proper information flow, whereas stimuli arriving out of phase would be less likely to elicit a response or be relayed forward [9–12]. Another consequence is the emergence of differential plasticity states, which are thought to occur through spike timing-dependent plasticity: presynaptic activity during high-excitability states, i.e., specific phases of a low-frequency oscillation, that are consistently followed by postsynaptic neuronal firing leads to strengthening of the synaptic connection. This may be of significant importance for cognition and memory formation, as synchronous activation of brain regions induces synaptic plasticity, allowing the neuronal system to hold items in memory [13,14]. In summary, these observations led to the suggestion that the dynamics of theta and fast oscillations, found in extended networks in the human brain, including prefrontal cortex, contribute significantly to the underpinnings of cognition [2,5,15].

Attempts have been made to interfere with these dynamics. *In vivo* studies of rat hippocampus found that stimulation during the positive peak of the ongoing theta oscillation in local field potentials led to long term potentiation, but to long term depression when the theta negative peak was stimulated [16,17]. When investigating behaving animals, theta phase-specific stimulation during task execution interfered with both the local oscillatory pattern and the animal's behavior, as phase-locked optogenetic inhibitory stimulation of hippocampus synchronized with the positive peak of the theta oscillation enhanced spatial memory retention, whereas stimulation coupled to the negative peak enhanced memory retrieval [18].

In humans, repetitive transcranial magnetic stimulation (rTMS) in high-frequency bursts (>30 Hz) at a low carrier frequency in the theta frequency range, a paradigm named theta burst stimulation, has been designed to simulate theta-gamma phase-amplitude coupling (PAC), which refers to the phenomenon of fast oscillatory neuronal activity (in the gamma frequency band) being nested in specific phases of a lower frequency oscillation (in the theta frequency band), as described above [19]. This paradigm has shown clinical improvement in experimental trials when compared to sham stimulation, although there are doubts of its superiority when compared to standard rTMS protocols [20], as well as challenges to its efficacy and reliability in modulating cortical responses [21]. One possible explanation for the lack of reliability of the method is that, despite the simulated theta-gamma coupling phenomenon, standard theta-burst stimulation does not take into account the instantaneous brain state at the time of stimulation, which might be of particular importance for effective cortical modulation. An alternative approach is attempting to entrain the cortex to oscillate in synchrony to an externally driven low-frequency oscillation by means of transcranial alternating current stimulation (tACS), while concomitantly applying gamma frequency band stimulation phase-locked to that entrained low frequency, which has provided evidence of positive effects on cortical responses and working memory modulation [22,23]. However, it is presently unclear to what extent tACS-entrained brain oscillations are equivalent to endogenous brain oscillations.

One study demonstrated that the retention of memory items can be modulated by TMS, depending on the phase of the endogenous prefrontal theta oscillation during which the pulses were applied, reinforcing the importance of the ongoing cortical state for TMS-induced behavioral effects [24]. The possibility of effectively modulating prefrontal cortical circuits operating in the theta band can have relevant implications for future studies of human cognition, including therapeutic applications in neuropsychiatric diseases associated with disordered brain networks and working memory (WM) [25,26].

In the present study, we attempted to interfere with neuronal networks in a state-dependent way in order to modulate cortical responsivity in behaving human subjects, defined as the capacity of consistently changing significant aspects of the electroencephalographic signature in response to stimuli. Towards this aim, rTMS was applied synchronized with ongoing oscillating brain-states analyzed with electroencephalography (EEG) in real time. We have previously introduced this approach in the human motor system, demonstrating that negative vs. positive peaks of the sensorimotor μ-rhythm (8–13 Hz) correspond to corticospinal high- vs. low-excitability states. Moreover, rTMS synchronized with the high-excitability state (negative peak) led to a long-term potentiation(LTP)-like increase in corticospinal excitability but not rTMS coupled to the low-excitability state (positive peak) or random-phase stimulation [27]. We have thereafter developed a similar approach to target specific phases of the prefrontal theta-oscillation [28]. Here we investigated to what extent rTMS coupled to specific phases of the prefrontal theta oscillation can differentially modulate cortical responsivity and behavior. For this purpose, we have chosen the dorsomedial prefrontal cortex (DMPFC) as the target for both extracting the theta oscillation and applying TMS, due to its role in both cognitive performance and generation of prefrontal theta rhythm [29,30]. As the scalp EEG negative peak of ongoing theta oscillations is associated with increased high-frequency neuronal activity in humans [2,12,31], we hypothesized that rTMS during the negative peak of the prefrontal theta oscillation will lead to increase in cortical responsivity probed by single-pulse TMS-EEG, represented by increased amplitude and power of the EEG responses, as well as improved performance in a WM task, when compared to the same stimulation at the positive peak or at random phase.

## 2. Methods

To test possible neuromodulatory effects of rTMS targeting the prefrontal cortex at specific phases of the local theta oscillation we conducted a study that included three experimental sessions consisting of three interventions of interest, each tested on different days. These included: rTMS with pulses applied either 1) during the negative peak of the ongoing theta oscillation, 2) during the positive peak or 3) at random phase. We tested different outcomes regarding cortical excitability using TMS-EEG, and behavior using a test of WM performance, measured prior and following each intervention. Details on these procedures are provided in the subsections below. Fig. 1 displays a visual representation of the experimental sessions.

A total of 22 healthy volunteers were included. Exclusion criteria were past or current psychiatric or neurological diseases, current treatment with drugs acting on the central nervous system, presence or prior history of alcohol or illicit drugs abuse, and current pregnancy. Four subjects were not included in the final analysis, two due to sleepiness during the experiments, and two due to excessive eye movements and scalp muscle contractions, which interfered with EEG signal analysis. Two further subjects did not participate in all sessions and were thus not included in the final analysis. The final sample consisted of 16 subjects (10 female) with a mean age of 23.4 years (S.D. ± 3.2). All subjects provided written informed consent prior to participation, and the study was performed in accord with the last version of the Declaration of Helsinki and approved by the ethics committee of the medical faculty of the University of Tübingen (716/2014BO2).

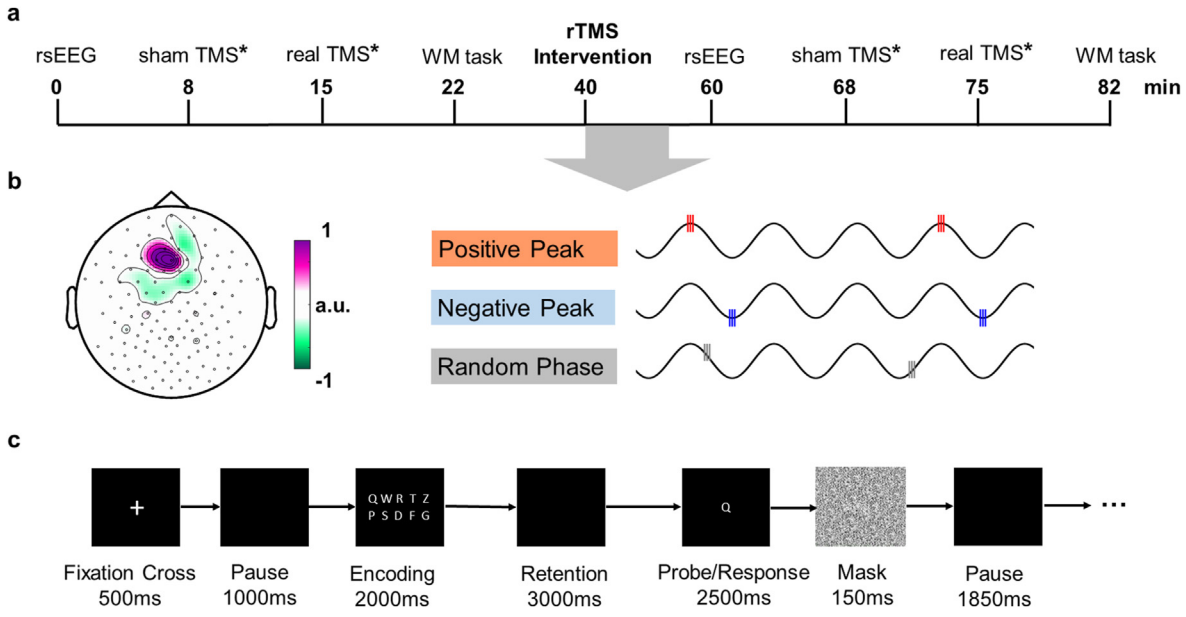


**Fig. 1. Visual representation of experimental sessions: a.** Experimental session timeline, displaying the time of the rTMS intervention, and the pre and post rTMS intervention measurements (* sham-controlled single-pulse TMS-EEG, to address peripheral evoked potentials in the TMS-EEG measurements evoked by real TMS). **b.** Illustration of the plasticity inducing rTMS interventions, with the topographical plot showing the coefficient weights (arbitrary units; a.u.) of the spatial filter in each electrode (average across all subjects; n = 16. Purple: positive values; green: negative values). Individualized filters were used to extract the signal from the left dorsomedial prefrontal cortex for each subject. To the right, the illustration shows application of 100 Hz triple pulses with relation to the ongoing theta-oscillation in each intervention: pulses applied phase-locked to the positive peak, phase-locked to the negative peak and random phase (i.e., not phase locked). **c.** Timeline of a single trial of the Sternberg working memory task (each measurement contained 100 trials before and 100 trials after the rTMS intervention), illustrating the screen display and duration of each step. Abbreviations: rsEEG, resting-state EEG; rTMS, repetitive TMS; WM, working memory. (For interpretation of the references to colour in this figure legend, the reader is referred to the Web version of this article.)

### 2.1. MRI and neuronavigation

Prior to the rTMS experimental sessions, subjects underwent ~~magnetic resonance imaging (MRI) using a 3T Siemens PRISMA scanner with T1- and T2-weighted anatomical sequences. A neuronavigation system (Localite GmbH, Sankt Augustin, Germany)~~ was used for targeting the desired cortical area with the TMS coil and maintaining the coil in a constant position relative to the participant's head throughout and across sessions.

The target for all TMS procedures was the left dorsomedial prefrontal cortex (DMPFC), identified by the Montreal Neurological Institute (MNI) coordinates −4, 52, 36 [32,33]. The coil orientation above the scalp was such that the vector of the induced electrical field on the cortex was perpendicular to the left superior frontal gyrus, with lateral to medial orientation. The coil was also placed atop a 11-mm plastic spacer mounted on the EEG electrodes, in order to prevent direct contact of the TMS coil with the electrodes to reduce possible artifacts [34], which was also present when determining the resting motor threshold (RMT) over motor cortex (see below).

### 2.2. Experimental set-up

Scalp EEG was recorded from a 126-channel TMS-compatible Ag/AgCl sintered ring electrode cap (EasyCap GmbH, Germany) in the International 10–5 EEG system arrangement [35]. A 24-bit biosignal amplifier was used for EEG and electromyography (EMG) recordings, with a recording rate of 5 kHz (NeurOne Tesla with Digital Out Option, Bittium Biosignals Ltd. Finland). Surface EMG was recorded for determination of RMT with standard methods, using bipolar EMG adhesive hydrogel electrodes (Kendall, Covidien) over the abductor pollicis brevis and first dorsal interosseus muscles of the right hand in a bipolar belly-tendon montage (5 kHz sampling rate, 0.16 Hz - 1.25 kHz bandpass filter) [36]. RMT was defined as the minimum TMS intensity to elicit a small motor evoked potential >50 μV in at least 5 out of 10 trials in at least one of the target muscles. The mean RMT was not different between rTMS interventions: 64% (S.D. ± 9.8) of the maximum stimulator output in the negative-peak intervention, 65% (S.D. ± 8.1) in the positive-peak intervention, and 65% (S.D. ± 8.9) in the random phase intervention.

Single-pulse TMS and rTMS were delivered using a MagPro XP Stimulator (MagVenture A/S, Denmark) connected to a figure-of-eight coil (Cool-B65, inner coil winding diameter 35 mm) using biphasic pulses of 300 μs width. For testing cortical neurophysiological effects (TMS-EEG), single-pulse TMS was used to probe EEG responses (real TMS condition). These measurements were also performed using a figure-of-eight sham coil (MCF-P-B65) attached to the same stimulator (sham condition) to control for potentials in the EEG response representing peripherally evoked potentials [37]. Additionally, subjects wore earbuds delivering masking noise, with sound pressure level individually adjusted to mask the TMS-induced click [38]. For WM testing, visual stimuli were delivered by an 80 × 35 cm curved LCD monitor placed 100 cm away from the subject's head. A response pad was connected to the EEG system for precise timing, marking the EEG traces with time and nature of the behavioral responses. This set-up was implemented with the open-source Matlab toolbox “Psychophysics Toolbox Version 3”.

### 2.3. EEG-triggered rTMS intervention

The study involved three distinct rTMS conditions in which the stimuli were applied during specific phases of the ongoing prefrontal theta-oscillation (see Fig. 1b): 1) phase-locked to the negative peak, 2) phase-locked to the positive peak, 3) random phase (i.e., not phase-locked). The order in which each protocol was applied was randomized and balanced across subjects, and subjects were blinded to the rTMS condition.

The prefrontal theta-oscillation was obtained by applying an individualized EEG spatial filter designed to extract the signal from each subject's left DMPFC, taking into consideration the individual cortical anatomy and the actual position of the EEG electrodes. To this end, individual MRIs were segmented and meshed using the FieldTrip toolbox [39], following the creation of a forward model for EEG using a customized pipeline [40,41]. Positions of all electrodes in each session were pinpointed manually using the neuronavigation system described above, and then projected onto the scalp surface mesh. A three-compartment volume conductor model was constructed using the boundary element method including intracranial space (conductivity 0.33 S/m), skull (0.0041 S/m), and scalp (0.33 S/m). Cortical source activity was represented as primary current density on the boundary of white and gray matters, discretized into approximately 16,000 source dipoles, each oriented perpendicular to the cortical surface. A linear constrained minimum variance (LCMV) beamformer was used to estimate the activity in source space [42]. Eight minutes of resting-state EEG (rsEEG, eyes open) were obtained at the beginning of each session for calculating the covariance matrix, required for the LCMV. The individual spatial filters were then obtained by selecting the columns of the resulting leadfield that corresponded to the dipoles located within 1 cm diameter centered in the left DMPFC (defined above), thus assigning a coefficient weight to each EEG channel (Fig. 1b). Further details on this procedure can be found in our previous publication [28].

For the rTMS interventions, phase-locked stimuli were controlled by a custom-built dedicated digital biosignal processor based on Simulink Real-Time, designed with an algorithm to perform EEG phase estimation and identify the phase of a specific frequency-band oscillation in real time [27]. EEG theta phase was estimated in real-time by downsampling the spatially filtered signal to 250 Hz and analyzing sliding windows of data with length of 256 samples, applying the following steps every 4 ms to yield an instantaneous phase estimate: (1) zero-phase filtering in both the forward and reverse directions with an FIR 5–8 Hz band-pass of order 80, (2) removal of 35 samples from the epoch's window closest to the marker in order to reduce filtering edge effects, (3) autoregressive forward, Yule-Walker method, prediction of order 15 and the total predicted interval of 268 ms (140 ms for the removed edge, and 128 ms into the future to avoid edge effects from the Hilbert transform), (4) Hilbert transform. TMS was triggered when the estimated phase corresponded to the target and two further conditions were met: a minimum of 1 s had passed since the previous stimulus, as to allow for accurate phase estimation undisturbed by the previous TMS artifact and TMS-evoked response, and no EEG signal artifacts were detected [28]. RTMS intensity was set to 120% of the RMT, a burst consisted of three pulses with 10 ms interstimulus interval (i.e., 100 Hz, first pulse centered on the target phase), with a total of 400 triplet bursts per session. The minimum interval between bursts was set to 1 s, with the exact inter-burst interval depending on the real-time phase-detection algorithm. The average of all inter–burst intervals was 3.49 s (S.D. ± 2.01 s) for the negative-peak intervention, 3.16 s (S.D. ± 2.11 s) for the positive-peak intervention, and 3.60 s (S.D. ± 2.00 s) for the random phase intervention (Kruskal–Wallis non-parametric analysis of variance: $p = 0.587$), resulting in an average duration of the rTMS interventions of approximately 21 min.

### 2.4. Outcome measures

EEG responses were obtained by applying a total of 160 single TMS pulses to the left DMPFC, prior and following each rTMS intervention. The coil placement was the same as for the rTMS interventions. TMS intensity was set to 120% of the RMT and interstimulus interval of 2.5 s (±0.5 s jitter). The triggering time for the single-pulse TMS-EEG was uncoupled to the phase of the ongoing theta oscillation or any other EEG signal (Fig. 1a).

Subjects also performed a modified Sternberg WM task [43] prior and following each rTMS intervention. The task involved the display of 10 random non-repeated consonant letters on a screen (encoding period), which subjects were instructed to keep in memory, followed by the display of a black screen for 3 s (retention period). Thereafter, a single letter was displayed on the screen and subjects had to respond whether this test letter was a member of the set of 10 letters previously shown ("true") or not ("false") by pushing a button on a panel held by the subjects. For the total 100 trials in each measurement, 50 trials were "true" (50%) and 50 trials were "false" (50%), occurring in randomized order. Accuracy of the response (accuracy) and time elapsed from probe letter display onset to button press (response time) were recorded, as well as the EEG signal during the task execution (Fig. 1c).

### 2.5. EEG data processing

*EEG preprocessing:* Offline data analysis was performed using the FieldTrip open source toolbox [39]. For analysis of TMS-evoked EEG potentials (TEPs), EEG data were segmented into epochs centered on the TMS pulse (−2000 to 2000 ms) and then baseline corrected (−500 to −50 ms). Data containing the TMS pulse and evoked scalp muscle activity (−2 to +18 ms window around each TMS pulse) were removed and cubic interpolated. Trials were inspected visually, epochs and channels with excessive noise were excluded, and further artifacts were removed with a 2-step independent component analysis procedure [44,45]. Lastly, excluded channels were spline-interpolated, and signals were then re-referenced to the average of all electrodes.

*TMS-induced oscillations:* For the processing of TMS-induced oscillations, time–frequency representations (TFRs) of TMS-related changes in oscillatory power were calculated using a Morlet wavelet decomposition on single trials [46], with frequency-dependent width (wavelet width of 2.6 cycles at 4 Hz, adding 0.2 cycle for each 1 Hz). The time–frequency oscillatory responses to TMS were divided into an evoked response (i.e., phase-locked to TMS) and an induced response (i.e., non-phase-locked to TMS) [47], followed by z-transforming the TFR of each trial with respect to the mean and standard deviation of the full trial, and baseline correction (−500 to −50 ms).

*Phase amplitude coupling (PAC):* For the estimation of PAC we calculated the Mean Vector Length (MVL) of the EEG response following each TMS pulse [48]. Morlet wavelet decomposition on single trials as described above was used to obtain a complex time frequency response, with epochs centered on the TMS pulse (−2000 to 2000 ms), followed by estimation of the phase angle from lower frequency bands (4–20 Hz), defined as the phase, and the power amplitude from higher frequency bands (20–90 Hz), defined as the amplitude [49]; performed for the time points from 0 to 1000 ms after the TMS pulse. The MVL was then calculated by the following formula:

$$MVL = \left| \frac{\sum_{t=1}^{n} a(t) e^{i\theta(t)}}{n} \right|$$

where $\boldsymbol{n}$ is the number of time points, $\boldsymbol{t}$ is a single time point, $\boldsymbol{a(t)}$ is the amplitude at a time point $\boldsymbol{t}$ and $\boldsymbol{\theta(t)}$ is the phase angle at the time point $\boldsymbol{t}$ [48,49]. The resulting MVL was then compared with surrogate datasets, created by randomly splitting the amplitude time course and shuffling it, while maintaining the phase time course, followed by the MVL calculation of the resulting signal. This

procedure was performed 200 times for each trial. The end result consists of the z-value obtained by subtracting from each trial the average of the surrogate control and divided by its standard deviation, thus standardizing the final result [49,50].

### 2.6. Statistical analyses

All statistical analyses were performed on the MATLAB platform (R2017b, The Mathworks, USA). Data were analyzed using all EEG channels, by means of non-parametric cluster-based permutation statistics, using the FieldTrip toolbox [39,51].

Behavioral outputs from the WM task, i.e., accuracy and response time, were compared using Mixed-Effects Models, which allow the inclusion of all the empirical observations in the model by including subject as random effect in the model. Fixed effects included were time (measurement pre or post intervention), intervention (negative peak, positive peak or random phase stimulation) and the interaction of time*intervention. Predictors were the reaction time, using a linear mixed-effects model, and accuracy ("true" or "false"), using a generalized linear mixed-effects model. In cases where the interaction time*intervention was found to significantly predict the outcome, the outcome measure was then averaged across trials per condition and submitted to dependent-variable t-tests in order to determine which intervention yielded a significant change to that outcome.

Statistical analyses of electrophysiological readouts extracted from the TMS-EEG recordings pose specific challenges due to the high dimensional multivariate nature of the data: multiple electrodes, time points and frequency bands (in the case of time-frequency analysis). This constitutes a considerable risk of false positive findings, if analyzing multiple dimensions or data points separately, but also false negative findings, when adjusting for multiple comparisons that are not independent. We therefore relied on non-parametric cluster based statistics designed for such multivariate EEG analyses, as provided by the FieldTrip toolbox [39,51].

Our first objective was to identify possible evidence that the modulatory effects of the rTMS interventions were different. Statistical analysis of TEPs involved a cluster-based ANOVA, using as input variables the difference of the TMS-EEG evoked responses before and after each of the 3 rTMS interventions (post-rTMS minus pre-rTMS), applying a threshold for cluster formation of 2 channels and $p < 0.025$, and including the period between 20 and 350 ms after the TMS-pulse probe. Statistically significant clusters, defined as displaying $p < 0.05$, were then *post hoc* tested by means of cluster-based *t*-tests for dependent samples, comparing the TEPs before and after each rTMS intervention, within the time windows in which the cluster was found. Effect sizes were calculated using Cohen's d of the amplitude of the averaged signal within the time window and channels of the respective significant cluster, and its 95% confidence interval.

For the TMS-induced oscillations the same cluster-based statistics procedure described for TEPs was used, but including the period of 50 ms–1000 ms after the TMS pulse. Moreover, for these analyses the data were *a priori* separated and averaged in predefined frequency bands of interest: theta (4–7 Hz), alpha (8–12 Hz), low beta (13–20 Hz), high beta (21–29 Hz), low gamma (30–45 Hz) and high gamma (60–90 Hz). Due to the multiple-testing nature of this procedure, the critical $\alpha$ level was adjusted to $p < 0.01$. A similar approach was used for the PAC statistics, setting *a priori* phases of theta (4–7 Hz) and alpha (8–12 Hz), while including the amplitudes (20–90Hz) in the permutation procedure, then requiring the critical $\alpha$ level adjustment to $p < 0.025$ for statistical significance.

Lastly, significant changes of behavioral outcome observed following a given intervention were compared to the changes in the TMS-EEG responses following the same intervention, by means of Pearson's correlation, using a critical $\alpha$ level appropriate for the number of comparisons, according to the Bonferroni correction.

## 3. Results

### 3.1. TMS evoked potentials

Potentials evoked by sham stimulation presented a pattern of signal deflections at around 100 ms and 200 ms after stimulation, while evoked potentials from real TMS presented a very similar pattern, with the addition of lower amplitude deflections at around 40 ms and 70 ms (Supplementary Material, Fig. S1). These patterns are similar to previous observations of EEG responses to TMS of the prefrontal cortex [44,52]. Cluster-based statistics did not reveal any significant cluster when comparing the EEG potentials evoked by sham or real TMS after vs. prior to any of the three rTMS interventions (Supplementary Material, Fig. S2), suggesting that none of the theta-phase specific rTMS interventions led to a significant change in TEPs.

### 3.2. TMS-induced oscillations

Cluster-based statistics demonstrated differential significant changes in oscillatory responses to single-pulse TMS after the rTMS interventions (Fig. 2). Specifically, the negative-peak rTMS intervention led to a significant increase in the power of the theta-band (latency 480–780 ms; cluster-based *t*-test: $t(15) = 4.35$, $p < 0.001$; Cohen's $d = 1.33$, $CI_{95\%} = [0.94, 1.72]$), alpha-band (latency 230–590 ms; cluster-based *t*-test: $t(15) = 4.21$, $p < 0.001$; Cohen's $d = 0.78$, $CI_{95\%} = [0.42, 1.15]$) and high gamma band (latency 260–340 ms; cluster-based *t*-test: $t(15) = 5.01$, $p < 0.001$; Cohen's $d = 1.17$, CI95% = [0.79, 1.55]). In contrast, the positive-peak intervention led to a significant decrease in the power of the theta-band (latency 90–970 ms; cluster-based *t*-test: $t(15) = -7.52$, $p < 0.001$; $d = 1.34$, $CI_{95\%} = [0.75, 1.52]$) and high beta-band responses (latency 470–820 ms; cluster-based *t*-test: $t(15) = -5.09$, $p < 0.001$; $d = 1.25$, $CI_{95\%} = [0.87, 1.64]$). No significant change was observed after the random phase rTMS intervention, despite a trend towards decreased theta power around 100–300 ms after the pulse (Fig. 2). This early-latency decrease in theta power suggests a common trend among the interventions, albeit of different magnitude, whereas distinct TMS-induced EEG signatures specific to the different interventions develop at longer latencies after the TMS pulse, as described above.

Furthermore, significant changes in the oscillations induced by sham TMS were not observed following any of the rTMS interventions, providing evidence that the effects observed with real TMS were not a result of modulation of non-specific sensory inputs (Supplementary Material, Fig. S3). Moreover, these results are unlikely accounted for by differences in the signals prior to the interventions, as there were no significant differences found between the pre-rTMS intervention responses (Supplementary Material, Fig. S4).

### 3.3. Phase amplitude coupling

Cluster-based statistics indicated significant changes in the TMS pulse induced PAC following the negative-peak rTMS intervention, found in the signal from electrodes over the medial prefrontal cortex (Fig. 3), with increase in the coupling of theta band phases and high gamma band amplitudes ($t(15) = 4.79$, $p < 0.001$; Cohen's

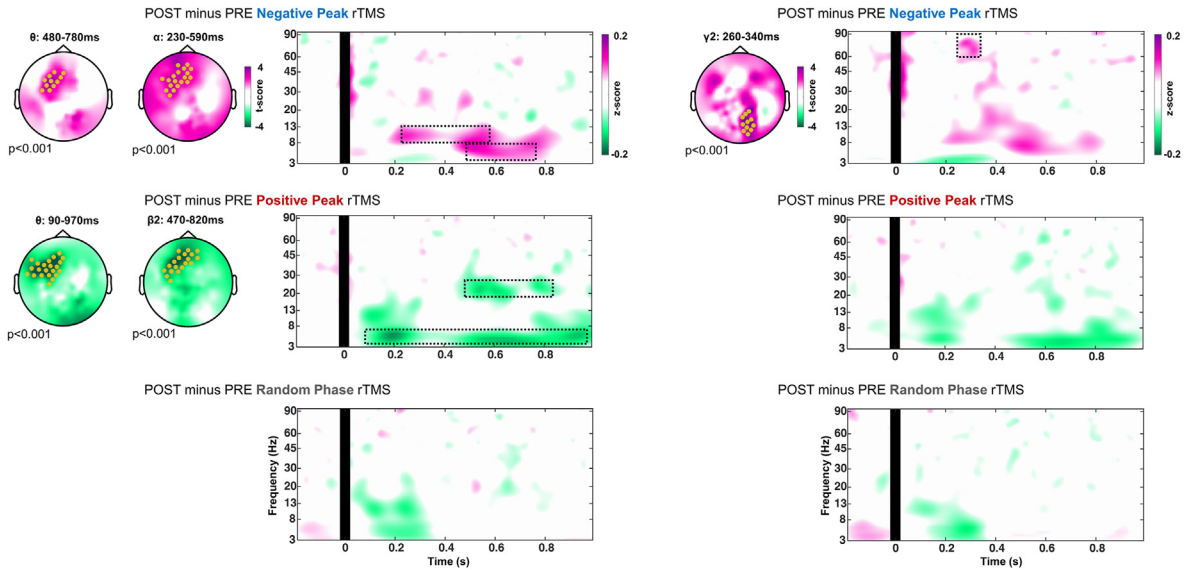


**Fig. 2. Differences between induced oscillations post minus pre rTMS intervention, divided by the interventions: negative peak; positive peak; and random phase.** Topographical plots show the statistically significant results from the pairwise comparison using cluster-based t-tests, with indications of the frequency band (θ: theta 4–7 Hz, α: alpha 8–12 Hz, β2: high beta 21–29 Hz, γ2: high gamma 60–90 Hz), and electrodes comprising the clusters highlighted as yellow dots. Time-frequency plots show the spectral power difference (post-rTMS minus pre-rTMS) tested by single-pulse TMS of the left dorsomedial prefrontal cortex, averaged across all subjects and the electrodes that composed the significant clusters. **Left** column plots show time-frequency plots averaged across all the common electrodes indicated on the topographical plots to the left, corresponding to anterior scalp regions close to the left dorsomedial prefrontal cortex targeted by the rTMS interventions. **Right** column plots show time-frequency plots averaged across electrodes indicated on the topographical plot to the left, corresponding to parieto-occipital cortex. Dotted black boxes indicate the periods and frequencies, in which the significant clusters were found. (For interpretation of the references to colour in this figure legend, the reader is referred to the Web version of this article.)

$d = 1.64$, $CI_{95\%} = [1.23, 2.05]$). No significant change was observed after either positive-peak or random phase rTMS intervention.

### 3.4. Accuracy and response time in the working memory task

The accuracy of all trials and response time of all trials followed a normal distribution (Shapiro–Wilk normality test, accuracy: $W(47) = 0.981$, $p = 0.645$; response time: $W(47) = 0.977$, $p = 0.495$), with distribution peaks distant from extreme values, pointing against a ceiling effect. We found no evidence for change in accuracy following any intervention. The generalized linear model for accuracy did not reveal significance of either the fixed effects *time* (pre-rTMS and post-rTMS measurements; $p = 0.965$), or *rTMS intervention* (negative peak, positive peak and random phase; $p = 0.441$) or the interaction *time*intervention* ($p = 0.447$). In contrast, the linear mixed effects model for response time found significance of *rTMS intervention* ($p = 0.041$), *time* ($p < 0.001$) and the interaction *time*intervention* ($p = 0.004$), with a *post hoc* analysis pointing to a significant decrease in response time following the negative-peak intervention (*t*-test: $t(15) = -2.94$, $p = 0.010$; $d = 0.49$, $CI_{95\%} = [0.13, 0.85]$), but no significant change following the positive-peak intervention (*t*-test: $t(15) = -0.21$, $p = 0.836$) or random-phase intervention (*t*-test: $t(15) = -0.47$, $p = 0.642$) (Fig. 4).

Furthermore, we observed an association between response accuracy and response time, with higher accuracies being associated with quicker response times (Fig. 4c). This is likely the result of confident responses being more promptly delivered. The rTMS intervention might have caused subjects to respond more impulsively, reducing the response time regardless of accuracy. We therefore repeated the analysis by only taking into consideration the response time for correct responses. The previous results were maintained, as the linear mixed effects model also revealed a significant interaction *time*intervention* ($p = 0.002$), with the *post hoc* analysis also pointing to a significant decrease in response time selectively following the negative peak intervention (*t*-test: $t(15) = -2.98$, $p = 0.009$; $d = 0.52$, $CI_{95\%} = [0.16, 0.88]$).

### 3.5. Correlation analyses between changes in working memory response time, TMS-induced oscillations and phase amplitude coupling

We found a non-significant trend towards an inverse correlation between changes in theta power and response time in the negative peak rTMS condition ($r = -0.52$; $p = 0.038$, Bonferroni corrected threshold $p < 0.006$), i.e., an increase in oscillatory theta power was associated with faster response times. No other significant correlations or trends were found (Fig. 5). Also concerning the negative peak rTMS condition, the prefrontal PAC increase was correlated to the increase in posterior high gamma response ($r = 0.68$; $p = 0.005$, Bonferroni corrected threshold $p < 0.006$), although we found no significant correlation with changes in working memory response time (Fig. 6).

## 4. Discussion

Our results suggest that rTMS of the dorsomedial prefrontal cortex with stimuli phase-locked to different phases of the local theta oscillation can differentially modulate cortical responsivity and performance in a working memory task. This corroborates and extends previous findings from slice preparations, animal experiments and recent studies in humans.

### 4.1. TMS-EEG

As hypothesized, rTMS phase-locked to the prefrontal theta oscillation significantly modulated cortical responses following the intervention. This was observed by an increased stimulus-induced oscillatory power of the theta band following rTMS phase-locked to the negative peak of the local theta oscillation, whereas positive

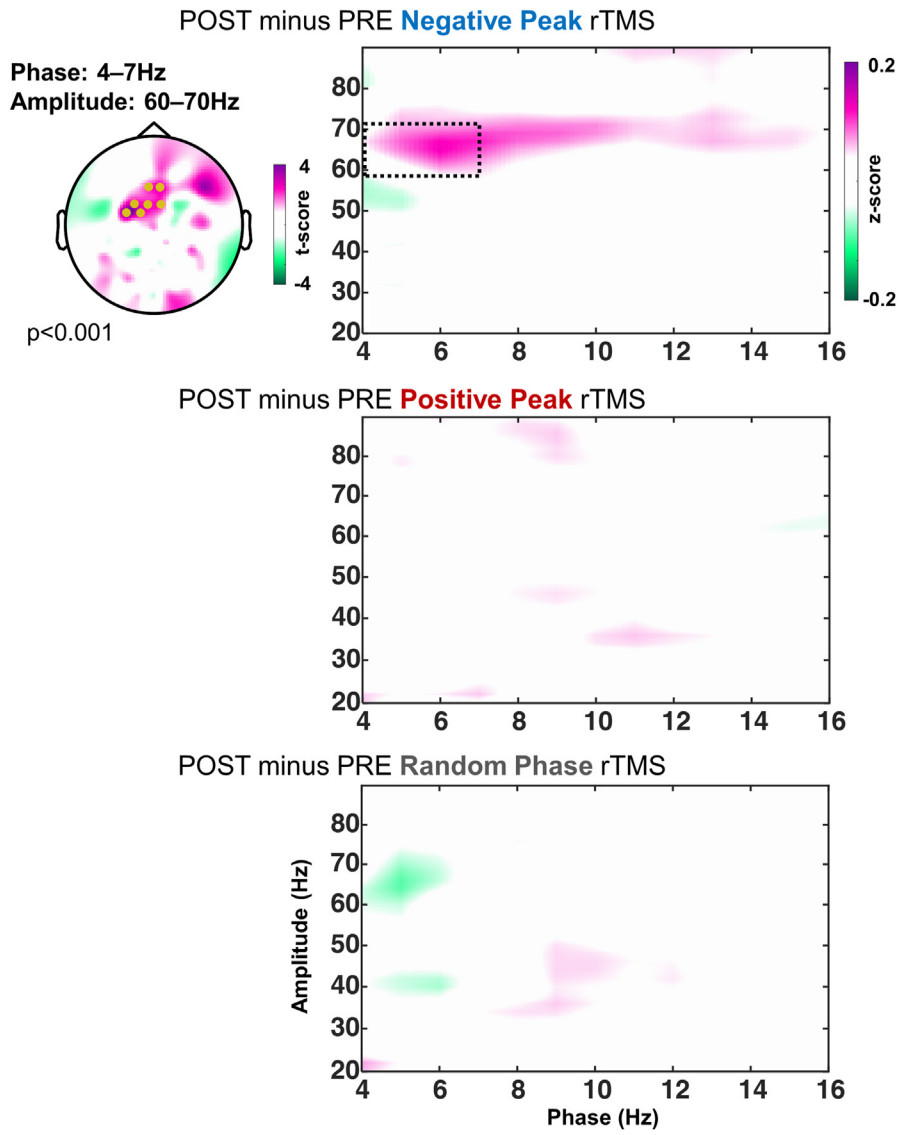


**Fig. 3. Differences between phase-amplitude coupling post minus pre rTMS intervention, divided by the interventions: negative peak; positive peak; and random phase. Left:** Topographical plot shows the statistically significant results in the negative-peak rTMS intervention from the pairwise comparison using cluster-based *t*-tests, and electrodes comprising the significant cluster highlighted as yellow dots. Phase and amplitude where the cluster was found and statistical significance are displayed next to the plot. **Right:** Comodulograms (phase of low-frequencies on the x-axis vs. amplitude of high-frequencies on the y-axis) show the coupling difference (post-rTMS minus pre-rTMS) averaged across all subjects and the electrodes that composed the significant cluster, displayed on the topographical plot to the left. Values displayed on the comodulograms correspond to the results of the mean vector length calculation, standardized (z-value) by surrogate data. Dotted black box indicates the period and frequency in which the significant cluster was found. (For interpretation of the references to colour in this figure legend, the reader is referred to the Web version of this article.)

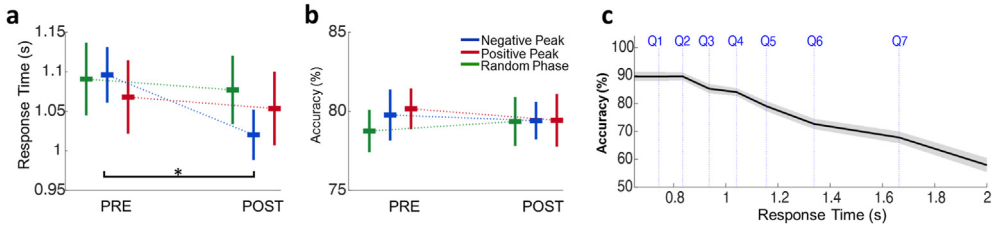


**Fig. 4. Behavioral outcomes of the working memory task:** Average response time (**a**) and accuracy (**b**) for the different interventions and measurements (pre-rTMS and post-rTMS). Central horizontal bars correspond to the mean and whiskers to standard error of the mean. * indicates statistically significant difference between the post-rTMS and pre-rTMS measurements ($p = 0.01$). **c.** Working memory task accuracy (shaded area corresponding to the standard error of the mean) plotted as a function of the response time, divided in quantiles (Q1-7), pooled from the pre-rTMS measurements across all three interventions.

peak rTMS led to a decrease in the theta-band response. These changes occurred specifically in cortical regions around the site of stimulation in the left prefrontal cortex, and in the targeted frequency band (Fig. 2). Oscillations induced by single-pulse TMS are

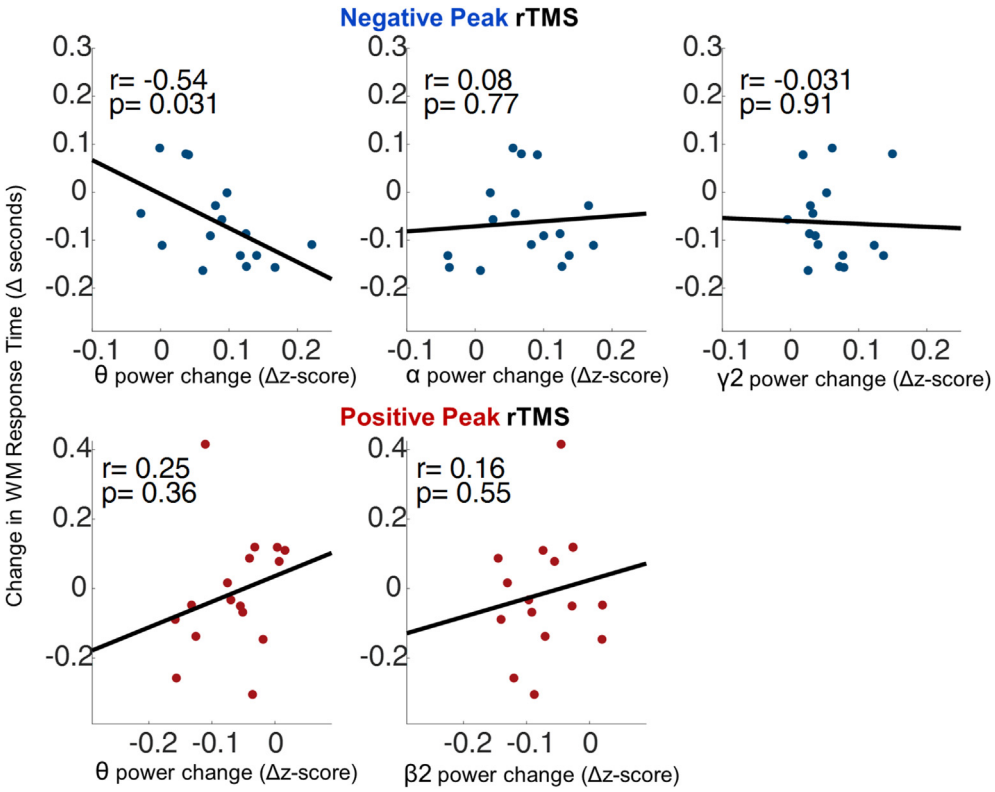


**Fig. 5. Correlations between changes in TMS-induced oscillations and reaction times in the negative peak and positive peak rTMS interventions.** Each dot corresponds to the results from one individual subject. Data on x-axes are Δ z-scores in EEG power in the indicated frequency bands post-rTMS minus pre-rTMS intervention. Data on y-axes are changes in reaction time (in seconds) post-rTMS minus pre-rTMS intervention. Each plot corresponds to data of a significant cluster from the TMS-induced oscillations (negative peak: θ theta 4–7 Hz from 480 to 780 ms, α alpha 8–12 Hz from 230 to 590 ms, and γ2 high gamma 60–90 Hz from 260 to 340 ms; positive peak: θ theta 4–7 Hz from 90 to 970 ms, and β2 high beta 21–29 Hz from 470 to 820 ms; cf. Fig. 2). Black lines are least-squares fit regression lines of the data from Pearson's correlation analysis.

thought to reflect the strength of naturally occurring activity of the stimulated cortex, as stimulation induces most prominent responses in the prevailing frequency band of that cortex. This is detected by the increased signal amplitude of that frequency band, which represents a larger number of cortical neurons activating in synchrony to that oscillation [53,54]. In the prefrontal cortex theta oscillations are prevalent, with significant physiological relevance for cognitive processing [7,55].

Of particular interest, the effects observed in this study occurred in the expected direction, with negative-peak rTMS enhancing theta oscillatory responses and positive-peak rTMS suppressing them. This result can potentially be explained by the nature of the corresponding interventions. Repetitive stimuli during a known state of higher excitability (i.e., the negative peak of the surface EEG theta oscillation, which is associated with higher likelihood of neuronal firing) is prone to lead a neuronal population to a sustained increase in responsivity to further stimuli, and opposite effects when stimuli occur during the state of lower cortical responsivity (i.e., positive peak) [14,16,56]. Moreover, the timing of these repetitive stimuli was by design phase-locked to the local ongoing theta oscillation, causing synchronous activation of neuronal populations specifically sensitive to excitability states determined by that oscillation. This might have led to the strengthening connections within the neuronal circuitries that

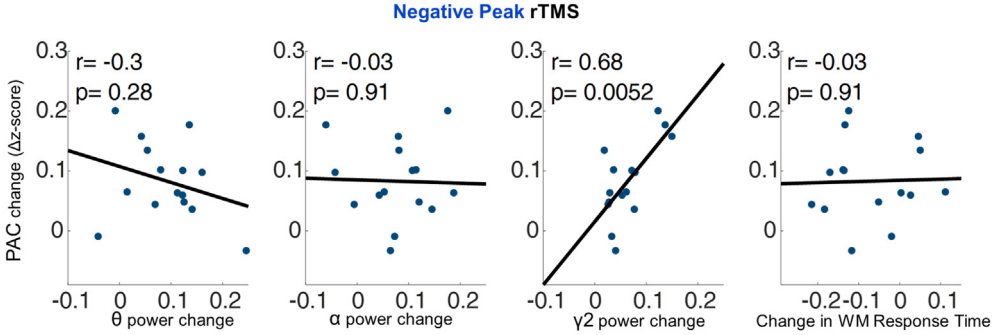


**Fig. 6. Correlations between changes in phase-amplitude coupling, TMS-induced oscillations and reaction times in the negative-peak rTMS intervention.** Each dot corresponds to the results from one individual subject. Data on x-axes are changes in power of induced oscillations post-rTMS minus pre-rTMS intervention (Δ z-scores), and change in WM response time in seconds (rightmost plot). Data on y-axes are changes in phase-amplitude coupling (Δ z-scores) post-rTMS minus pre-rTMS intervention. Black lines are least-squares fit regression lines of the data from Pearson's correlation analysis.

respond to theta oscillation, leading to a larger number of neurons reacting synchronously to incoming stimulus in that frequency band. The observable effect is the increased responsivity of the prefrontal cortex in the theta frequency band, measured with TMS-EEG, following repetitive stimulation during the theta high-excitability phase.

The lack of a significant effect from rTMS applied at random phase corroborates the relevance of phase-specific stimulation in promoting these neuromodulatory effects. Nevertheless, this condition resulted in a trend towards a decreased theta power response at early latencies (up to 300 ms after the TMS pulse, Fig. 2), which, to a lesser extent, was also observed after the negative-peak intervention, and reached significance after the positive-peak intervention. Corresponding effects have been described following other neuromodulatory interventions, including TBS [57,58], transcranial direct current stimulation [59] and magneto- and electroconvulsive therapy [60], suggesting that decreased early theta power responsivity to single-pulse TMS might correspond to an unspecific effect of prefrontal cortex stimulation. A possible complementary explanation is that early TMS responses in the theta band represent peripherally evoked responses caused by the multisensory input from TMS [61], which adds to the low specificity of the observed effect. This is supported by the results of probing cortical responsivity with sham stimulation, which also induced an early theta response (Supplementary Fig. 3). In the responses to real TMS, these effects were followed by diverging TMS-EEG signatures at later latencies, which were specific to the different interventions (cf. Fig. 2). By using a TMS sham control for peripherally evoked responses, Herring et al. observed that occipital cortex TMS evokes increased alpha oscillatory activity for up to 800 ms after the pulse, a frequency mode predominant in that cortical region, with positive cortical state modulatory effects [54]. These findings provide additional evidence that modulation of oscillatory responses specific to the cortical region of interest can involve latencies beyond 300 ms after the TMS pulse.

Importantly, the bursts of rTMS consisted of pulses in the gamma-frequency range (100 Hz), which were synchronized to either the negative or positive peak of the ongoing prefrontal theta oscillation, simulating theta–gamma PAC. Theta-gamma PAC, with gamma nested in the negative phase of the theta oscillation, occurs in large-scale cortico–thalamo–cortical, cortico–cortical, and cortico–hippocampal networks during information encoding and retrieval, providing a general mechanism underlying synaptic plasticity and memory formation [2,12–14,62,63]. The present findings are also in line with our previous observations in human motor cortex that gamma-burst rTMS resulted in an LTP-like increase in excitability of the corticospinal projection, but only if synchronized to the negative peak of the ongoing μ-oscillation, a high-excitability state of the corticospinal system [27]. Likewise, the negative peak rTMS intervention was also responsible for increasing the strength of the endogenous theta-gamma PAC in the stimulated DMPFC (cf. Fig. 3), further suggesting that the procedure is differentially modulating prefrontal circuits involved in local theta oscillation dynamics. One objection is that, although there is previous evidence suggesting that cortical stimulation applying similar theta-phase nested gamma-frequency ranges (80–100 Hz) by using cross-frequency tACS might be optimal for modulating prefrontal cortex responsivity [22,23], it is not clear whether this can be translated directly to the present method, nor whether this is a necessary condition to increase endogenous theta-gamma PAC. Further studies would be required to test possible roles and parameters for the nested gamma-frequency TMS bursts in this experimental setting of prefrontal theta-phase dependent induced plasticity.

Moreover, theta phase-specific rTMS also modulated oscillations in other frequency bands depending on the rTMS intervention (Fig. 2). This might indicate a complex interaction between oscillatory circuitries in the frontal cortex. Responses to prefrontal cortex stimulation also involve induced oscillatory activity in the high beta band (20–29 Hz) that corresponds to a stimulation site-specific reactive tuning of the corticothalamic circuits [53]. Modulation of beta oscillations in the prefrontal cortex has been shown to disrupt WM, and beta activity has been suggested to represent brain states distinct from theta–gamma [64,65]. In this line, alpha and beta activity in the prefrontal cortex has been associated with further functions including control inhibition tasks, behavior maintenance and rule-oriented behavior [30,66,67]. These cognitive functions might also be affected by the theta phase-specific rTMS, although this was not tested in the present study and further investigations would be necessary to explore this hypothesis. Of note, only the positive-peak rTMS intervention led to significant modulation (i.e., a decrease) of this oscillatory response in the high beta band. Although prefrontal alpha has also been associated with relevant cognitive functions, the results observed here (i.e., the increase specifically observed in the negative-peak rTMS intervention) might have been confounded by the close boundaries between the theta and alpha frequencies bands. Some studies suggested that theta can be divided into low-theta, predominantly found in hippocampus, and high-theta, with an average frequency of 7 Hz in prefrontal regions [68,69]. As we have employed the classical boundaries between theta (4–7 Hz) and alpha (8–12 Hz), the possibility must be considered that the observed increase in the theta/alpha bands specifically following the negative-peak rTMS intervention is centered on this boundary and reflects largely the high-theta band, i.e., the specific oscillation of the prefrontal cortex. Lastly, the negative-peak rTMS intervention led to a distant effect, namely the increase in gamma responsivity in posterior regions. This is concordant with the role of prefrontal theta oscillation in coordinating high-frequency neuronal activity in posterior cortical regions [2,4]. Therefore, the increased responsivity of the prefrontal circuits responding to theta oscillation might also result in the increased posterior gamma responsivity through fronto-posterior networks [70]. This is further supported by the positive correlation between the increases of gamma responsivity in the posterior cortical region and prefrontal theta-gamma PAC (cf. Fig. 6).

Contrary to our expectations, no significant changes in TEPs were observed following the rTMS interventions. This suggests that TEP amplitudes might be insensitive to the effects of theta phase-locked rTMS of prefrontal cortex. Of note, other studies that have examined rTMS effects in motor cortex did not show changes in TEPs either, despite significant changes of other cortical excitability markers, i.e., the motor evoked potential amplitude [71,72].

### 4.2. Working memory task

Several studies have investigated the possible effects of non-invasive brain stimulation on WM performance. A meta-analysis that pooled studies using rTMS for WM improvement suggested that, despite most studies not having found significant effects, the pooled analysis showed an overall positive effect (i.e., an increase in accuracy and a decrease of response time) from those rTMS interventions that aimed at increasing cortical excitability [73]. The present work also demonstrates that phase-specific rTMS differentially modulated WM performance, with rTMS applied during the negative peak of the ongoing theta oscillation significantly shortening response time (Fig. 3). A direct comparison would be needed to test whether theta phase-specific rTMS as applied in the present study is more effective than other methods in enhancing cognitive control in WM tasks.

Our findings are also in agreement with results from other brain stimulation studies that aimed at modulating theta activity, with WM response time reduction following prefrontal theta burst stimulation and theta-frequency transcranial alternating electrical stimulation (tACS) [74–76]. Modulation of prefrontal theta oscillation power is expected to alter WM response time, with increased theta power correlated with faster and more efficient WM processing, and considered as a marker of effective cognitive control [77]. Accordingly, we found a trend towards an inverse correlation between changes in single-pulse TMS-induced theta power and response time, specific to the negative-peak rTMS condition, i.e., an increase in oscillatory theta power was associated with faster response times (Fig. 4). The limited statistical significance of this finding might be explained by the modest effect size of the negative-peak rTMS-induced decrease of WM response time. One reason for the limited effect size of these outcomes is likely the testing of healthy subjects with neuronal network already working at or close to optimal capacity [78]. Another limitation is that the rTMS interventions were applied during rest. It is possible that the interventions were successful in differentially modulating networks dependent on theta activity, as observed by their differential effects on single-pulse TMS-induced EEG responses, but might not have been optimal for modulating the specific circuitry responsible for WM performance. As a consequence, despite the present intervention leading to correlated changes in prefrontal theta-gamma PAC and posterior gamma responsivity, these seem to have no sway over WM output in the present study. A possible approach to test this could be applying neuromodulatory techniques during the execution of a particular task, thereby potentially increasing the likelihood that the neural mechanisms modulated are the ones responsible for the task's execution, as has been suggested by previous reports showing trends towards stronger effect sizes. Of note, this seems to be the case only when the intervention is tailored to the network of interest (e.g., tACS in the theta frequency of the prefrontal cortex) [68,79], but not for non-specific interventions (e.g., transcranial direct current stimulation, rTMS not tuned to the frequency of specific interest) [80,81]. The use of theta-phase specific rTMS during the execution of behavioral tasks may prove to further increase the modulatory effects over neuronal circuits and behavioral performance associated with this oscillatory activity, but this will need further exploration in future studies.

## 5. Conclusions

We demonstrated that the novel EEG-rTMS technology significantly modulated the prefrontal theta oscillation and its related behavioral functions in a working memory task. In accord with recent experimental data, the present results can be explained by phase-specific theta–gamma phase–amplitude coupling in the prefrontal neuronal circuitry, which underlies working memory processes. The EEG-rTMS technology can potentially enrich the scientific inquiry of the physiological underpinnings of cognition in humans. More importantly, we and others believe that exploitation of theta–gamma phase–amplitude coupling has the potential to alleviate working memory impairment in individuals suffering from neuropsychiatric disorders.

## CRediT authorship contribution statement

**Pedro Caldana Gordon:** Conceptualization, Formal analysis, Writing – original draft, Conception or design of the work, Data analysis and interpretation, Data collection, Drafting the article, Final approval of the version to be published: all authors. **Paolo Belardinelli:** Conceptualization, Formal analysis, Writing – original draft, Data analysis and interpretation, Final approval of the version to be published: all authors. **Matti Stenroos:** Conceptualization, Formal analysis, Writing – original draft, Data analysis and interpretation, Final approval of the version to be published: all authors. **Ulf Ziemann:** Conceptualization, Formal analysis, Writing – original draft, Conception or design of the work, Data analysis and interpretation, Critical revision of the article, Final approval of the version to be published: all authors. **Christoph Zrenner:** Conceptualization, Formal analysis, Writing – original draft, Conception or design of the work, Data analysis and interpretation, Critical revision of the article, Final approval of the version to be published: all authors.

## Declaration of cpmpeting interest

The authors declare that they have no known competing financial interests or personal relationships that could have appeared to influence the work reported in this paper.

The authors declare the following financial interests/personal relationships which may be considered as potential competing interests: Christoph Zrenner reports an interest in and part-time work for a start-up company, sync2brain GmbH, which commercializes the real-time EEG analysis technology used in this study.

Pedro Caldana Gordon, Paolo Belardinelli, Matti Stenroos and Ulf Ziemann have no competing financial interests or personal relationships that could have appeared to influence the work reported in this paper.

## Acknowledgements

The authors are grateful for administrative support by Anna Kempf and Dragana Galevska, and help with the beamforming software by Dr. Natalie Schaworonkow.

C.Z. acknowledges support from the Clinician Scientist Program at the Faculty of Medicine at the University of Tübingen. P.C.G. and C. Z. report funding through the EXIST translational research program from the German Federal Ministry for Economic Affairs and Energy (grant 03EFJBW169). Furthermore, this project has received funding to U.Z. from the European Research Council (ERC) under the European Union's Horizon 2020 research and innovation programme (ConnectToBrain, ERC synergy grant agreement No 810377).

## Appendix A. Supplementary data

Supplementary data to this article can be found online at https://doi.org/10.1016/j.brs.2022.02.006.

## References

[1] Buzsaki G, Draguhn A. Neuronal oscillations in cortical networks. Science 2004;304(5679):1926–9.
[2] Cavanagh JF, Frank MJ. Frontal theta as a mechanism for cognitive control. Trends Cognit Sci 2014;18(8):414–21.
[3] Lisman J, Buzsaki G. A neural coding scheme formed by the combined function of gamma and theta oscillations. Schizophr Bull 2008;34(5):974–80.
[4] Sauseng P, Griesmayr B, Freunberger R, Klimesch W. Control mechanisms in working memory: a possible function of EEG theta oscillations. Neurosci Biobehav Rev 2010;34(7):1015–22.
[5] Fries P. Rhythms for cognition: communication through coherence. Neuron 2015;88(1):220–35.
[6] Gevins A, Smith ME, McEvoy L, Yu D. High-resolution EEG mapping of cortical activation related to working memory: effects of task difficulty, type of processing, and practice. Cerebr Cortex 1997;7(4):374–85.
[7] Onton J, Delorme A, Makeig S. Frontal midline EEG dynamics during working memory. Neuroimage 2005;27(2):341–56.
[8] Sauseng P, Hoppe J, Klimesch W, Gerloff C, Hummel FC. Dissociation of sustained attention from central executive functions: local activity and interregional connectivity in the theta range. Eur J Neurosci 2007;25(2):587–93.

[9] Benchenane K, Peyrache A, Khamassi M, Tierney PL, Gioanni Y, Battaglia FP, et al. Coherent theta oscillations and reorganization of spike timing in the hippocampal- prefrontal network upon learning. Neuron 2010;66(6):921–36.
[10] Fujisawa S, Buzsaki G. A 4 Hz oscillation adaptively synchronizes prefrontal, VTA, and hippocampal activities. Neuron 2011;72(1):153–65.
[11] Jones MW, Wilson MA. Theta rhythms coordinate hippocampal-prefrontal interactions in a spatial memory task. PLoS Biol 2005;3(12):e402.
[12] Rutishauser U, Ross IB, Mamelak AN, Schuman EM. Human memory strength is predicted by theta-frequency phase-locking of single neurons. Nature 2010;464(7290):903–7.
[13] Fell J, Axmacher N. The role of phase synchronization in memory processes. Nat Rev Neurosci 2011;12(2):105–18.
[14] Bergmann TO, Born J. Phase-amplitude coupling: a general mechanism for memory processing and synaptic plasticity? Neuron 2018;97(1):10–3.
[15] Mitchell DJ, McNaughton N, Flanagan D, Kirk IJ. Frontal-midline theta from the perspective of hippocampal "theta. Prog Neurobiol 2008;86(3):156–85.
[16] Hyman JM, Wyble BP, Goyal V, Rossi CA, Hasselmo ME. Stimulation in hippocampal region CA1 in behaving rats yields long-term potentiation when delivered to the peak of theta and long-term depression when delivered to the trough. J Neurosci 2003;23(37):11725–31.
[17] Orr G, Rao G, Houston FP, McNaughton BL, Barnes CA. Hippocampal synaptic plasticity is modulated by theta rhythm in the fascia dentata of adult and aged freely behaving rats. Hippocampus 2001;11(6):647–54.
[18] Siegle JH, Wilson MA. Enhancement of encoding and retrieval functions through theta phase-specific manipulation of hippocampus. Elife 2014;3:e03061.
[19] Huang YZ, Edwards MJ, Rounis E, Bhatia KP, Rothwell JC. Theta burst stimulation of the human motor cortex. Neuron 2005;45(2):201–6.
[20] Blumberger DM, Vila-Rodriguez F, Thorpe KE, Feffer K, Noda Y, Giacobbe P, et al. Effectiveness of theta burst versus high-frequency repetitive transcranial magnetic stimulation in patients with depression (THREE-D): a randomised non-inferiority trial. Lancet 2018;391(10131):1683–92.
[21] Ozdemir RA, Boucher P, Fried PJ, Momi D, Jannati A, Pascual-Leone A, et al. Reproducibility of cortical response modulation induced by intermittent and continuous theta-burst stimulation of the human motor cortex. Brain Stimul 2021;14(4):949–64.
[22] Alekseichuk I, Turi Z, Amador de Lara G, Antal A, Paulus W. Spatial working memory in humans depends on theta and high gamma synchronization in the prefrontal cortex. Curr Biol 2016;26(12):1513–21.
[23] Hosseinian T, Yavari F, Kuo MF, Nitsche MA, Jamil A. Phase synchronized 6 Hz transcranial electric and magnetic stimulation boosts frontal theta activity and enhances working memory. Neuroimage 2021;245:118772.
[24] Berger B, Griesmayr B, Minarik T, Biel AL, Pinal D, Sterr A, et al. Dynamic regulation of interregional cortical communication by slow brain oscillations during working memory. Nat Commun 2019;10(1):4242.
[25] Goodman MS, Kumar S, Zomorrodi R, Ghazala Z, Cheam ASM, Barr MS, et al. Theta-gamma coupling and working memory in alzheimer's dementia and mild cognitive impairment. Front Aging Neurosci 2018;10:101.
[26] Sigurdsson T, Stark KL, Karayiorgou M, Gogos JA, Gordon JA. Impaired hippocampal-prefrontal synchrony in a genetic mouse model of schizophrenia. Nature 2010;464(7289):763–7.
[27] Zrenner C, Desideri D, Belardinelli P, Ziemann U. Real-time EEG-defined excitability states determine efficacy of TMS-induced plasticity in human motor cortex. Brain Stimul 2018;11(2):374–89.
[28] Gordon P, Dörre S, Belardinelli P, Stenroos M, Zrenner B, Ziemann U, et al. Prefrontal theta-phase synchronized brain stimulation with real-time EEG-triggered TMS. Front Hum Neurosci 2021:15.
[29] Tsujimoto T, Shimazu H, Isomura Y, Sasaki K. Theta oscillations in primate prefrontal and anterior cingulate cortices in forewarned reaction time tasks. J Neurophysiol 2010;103(2):827–43.
[30] Zavala B, Jang A, Trotta M, Lungu CI, Brown P, Zaghloul KA. Cognitive control involves theta power within trials and beta power across trials in the prefrontal-subthalamic network. Brain 2018;141(12):3361–76.
[31] Tang W, Liu H, Douw L, Kramer MA, Eden UT, Hamalainen MS, et al. Dynamic connectivity modulates local activity in the core regions of the default-mode network. Proc Natl Acad Sci U S A 2017;114(36):9713–8.
[32] Dunlop K, Gaprielian P, Blumberger D, Daskalakis ZJ, Kennedy SH, Giacobbe P, et al. MRI-guided dmPFC-rTMS as a treatment for treatment-resistant major depressive disorder. JoVE 2015;(102):e53129.
[33] Piva M, Velnoskey K, Jia R, Nair A, Levy I, Chang SW. The dorsomedial prefrontal cortex computes task-invariant relative subjective value for self and other. Elife 2019;8.
[34] Ruddy KL, Woolley DG, Mantini D, Balsters JH, Enz N, Wenderoth N. Improving the quality of combined EEG-TMS neural recordings: introducing the coil spacer. J Neurosci Methods 2018;294:34–9.
[35] Oostenveld R, Praamstra P. The five percent electrode system for high-resolution EEG and ERP measurements. Clin Neurophysiol 2001;112(4):713–9.
[36] Groppa S, Oliviero A, Eisen A, Quartarone A, Cohen LG, Mall V, et al. A practical guide to diagnostic transcranial magnetic stimulation: report of an IFCN committee. Clin Neurophysiol 2012;123(5):858–82.
[37] Conde V, Tomasevic L, Akopian I, Stanek K, Saturnino GB, Thielscher A, et al. The non-transcranial TMS-evoked potential is an inherent source of ambiguity in TMS-EEG studies. Neuroimage 2019;185:300–12.
[38] Massimini M, Ferrarelli F, Huber R, Esser SK, Singh H, Tononi G. Breakdown of cortical effective connectivity during sleep. Science 2005;309(5744):2228–32.
[39] Oostenveld R, Fries P, Maris E, Schoffelen JM. FieldTrip: open source software for advanced analysis of MEG, EEG, and invasive electrophysiological data. Comput Intell Neurosci 2011:156869. 2011.
[40] Stenroos M, Sarvas J. Bioelectromagnetic forward problem: isolated source approach revis(it). Phys Med Biol 2012;57(11):3517–35.
[41] Stenroos M, Nummenmaa A. Incorporating and compensating cerebrospinal fluid in surface-based forward models of magneto- and electroencephalography. PLoS One 2016;11(7):e0159595.
[42] Van Veen BD, van Drongelen W, Yuchtman M, Suzuki A. Localization of brain electrical activity via linearly constrained minimum variance spatial filtering. IEEE Trans Biomed Eng 1997;44(9):867–80.
[43] Segrave RA, Thomson RH, Cooper NR, Croft RJ, Sheppard DM, Fitzgerald PB. Upper alpha activity during working memory processing reflects abnormal inhibition in major depression. J Affect Disord 2010;127(1–3):191–8.
[44] Rogasch NC, Thomson RH, Farzan F, Fitzgibbon BM, Bailey NW, Hernandez-Pavon JC, et al. Removing artefacts from TMS-EEG recordings using independent component analysis: importance for assessing prefrontal and motor cortex network properties. Neuroimage 2014;101:425–39.
[45] Rogasch NC, Sullivan C, Thomson RH, Rose NS, Bailey NW, Fitzgerald PB, et al. Analysing concurrent transcranial magnetic stimulation and electroencephalographic data: a review and introduction to the open-source TESA software. Neuroimage 2017;147:934–51.
[46] Tallon-Baudry C, Bertrand O. Oscillatory gamma activity in humans and its role in object representation. Trends Cognit Sci 1999;3(4):151–62.
[47] Premoli I, Bergmann TO, Fecchio M, Rosanova M, Biondi A, Belardinelli P, et al. The impact of GABAergic drugs on TMS-induced brain oscillations in human motor cortex. Neuroimage 2017;163:1–12.
[48] Canolty RT, Edwards E, Dalal SS, Soltani M, Nagarajan SS, Kirsch HE, et al. High gamma power is phase-locked to theta oscillations in human neocortex. Science 2006;313(5793):1626–8.
[49] Hulsemann MJ, Naumann E, Rasch B. Quantification of phase-amplitude coupling in neuronal oscillations: comparison of phase-locking value, mean vector length, modulation index, and generalized-linear-modeling-cross-frequency-coupling. Front Neurosci 2019;13:573.
[50] Munia TTK, Aviyente S. Time-frequency based phase-amplitude coupling measure for neuronal oscillations. Sci Rep 2019;9(1):12441.
[51] Maris E, Oostenveld R. Nonparametric statistical testing of EEG- and MEG-data. J Neurosci Methods 2007;164(1):177–90.
[52] Biabani M, Fornito A, Mutanen TP, Morrow J, Rogasch NC. Characterizing and minimizing the contribution of sensory inputs to TMS-evoked potentials. Brain Stimul 2019;12(6):1537–52.
[53] Rosanova M, Casali A, Bellina V, Resta F, Mariotti M, Massimini M. Natural frequencies of human corticothalamic circuits. J Neurosci 2009;29(24):7679–85.
[54] Herring JD, Thut G, Jensen O, Bergmann TO. Attention modulates TMS-locked alpha oscillations in the visual cortex. J Neurosci 2015;35(43):14435–47.
[55] Jensen O, Tesche CD. Frontal theta activity in humans increases with memory load in a working memory task. Eur J Neurosci 2002;15(8):1395–9.
[56] Cummings JA, Mulkey RM, Nicoll RA, Malenka RC. Ca2+ signaling requirements for long-term depression in the hippocampus. Neuron 1996;16(4):825–33.
[57] Bai Z, Zhang J, Fong KNK. Intermittent theta burst stimulation to the primary motor cortex reduces cortical inhibition: a TMS-EEG study. Brain Sci 2021;11(9).
[58] Chung SW, Lewis BP, Rogasch NC, Saeki T, Thomson RH, Hoy KE, et al. Demonstration of short-term plasticity in the dorsolateral prefrontal cortex with theta burst stimulation: a TMS-EEG study. Clin Neurophysiol 2017;128(7):1117–26.
[59] Gordon PC, Zrenner C, Desideri D, Belardinelli P, Zrenner B, Brunoni AR, et al. Modulation of cortical responses by transcranial direct current stimulation of dorsolateral prefrontal cortex: a resting-state EEG and TMS-EEG study. Brain Stimul 2018.
[60] Hill AT, Hadas I, Zomorrodi R, Voineskos D, Fitzgerald PB, Blumberger DM, et al. Characterizing cortical oscillatory responses in major depressive disorder before and after convulsive therapy: a TMS-EEG study. J Affect Disord 2021;287:78–88.
[61] Gordon PC, Jovellar DB, Song Y, Zrenner C, Belardinelli P, Siebner HR, et al. Recording brain responses to TMS of primary motor cortex by EEG - utility of an optimized sham procedure. Neuroimage 2021;245:118708.
[62] Lisman JE, Jensen O. The theta-gamma neural code. Neuron 2013;77(6):1002–16.
[63] Womelsdorf T, Vinck M, Leung LS, Everling S. Selective theta-synchronization of choice-relevant information subserves goal-directed behavior. Front Hum Neurosci 2010;4:210.
[64] Hanslmayr S, Matuschek J, Fellner MC. Entrainment of prefrontal beta oscillations induces an endogenous echo and impairs memory formation. Curr Biol 2014;24(8):904–9.
[65] Lundqvist M, Rose J, Herman P, Brincat SL, Buschman TJ, Miller EK. Gamma and beta bursts underlie working memory. Neuron 2016;90(1):152–64.
[66] Buschman TJ, Denovellis EL, Diogo C, Bullock D, Miller EK. Synchronous oscillatory neural ensembles for rules in the prefrontal cortex. Neuron 2012;76(4):838–46.

[67] Engel AK, Fries P. Beta-band oscillations–signalling the status quo? Curr Opin Neurobiol 2010;20(2):156–65.
[68] Wolinski N, Cooper NR, Sauseng P, Romei V. The speed of parietal theta frequency drives visuospatial working memory capacity. PLoS Biol 2018;16(3):e2005348.
[69] Goyal A, Miller J, Qasim SE, Watrous AJ, Zhang H, Stein JM, et al. Functionally distinct high and low theta oscillations in the human hippocampus. Nat Commun 2020;11(1):2469.
[70] Chung SW, Sullivan CM, Rogasch NC, Hoy KE, Bailey NW, Cash RFH, et al. The effects of individualised intermittent theta burst stimulation in the prefrontal cortex: a TMS-EEG study. Hum Brain Mapp 2019;40(2):608–27.
[71] Gedankien T, Fried PJ, Pascual-Leone A, Shafi MM. Intermittent theta-burst stimulation induces correlated changes in cortical and corticospinal excitability in healthy older subjects. Clin Neurophysiol 2017;128(12):2419–27.
[72] Desideri D, Zrenner C, Gordon PC, Ziemann U, Belardinelli P. Nil effects of mu-rhythm phase-dependent burst-rTMS on cortical excitability in humans: a resting-state EEG and TMS-EEG study. PLoS One 2018;13(12):e0208747.
[73] Brunoni AR, Vanderhasselt MA. Working memory improvement with non-invasive brain stimulation of the dorsolateral prefrontal cortex: a systematic review and meta-analysis. Brain Cognit 2014;86:1–9.
[74] Chung SW, Rogasch NC, Hoy KE, Sullivan CM, Cash RFH, Fitzgerald PB. Impact of different intensities of intermittent theta burst stimulation on the cortical properties during TMS-EEG and working memory performance. Hum Brain Mapp 2017.
[75] Polania R, Nitsche MA, Korman C, Batsikadze G, Paulus W. The importance of timing in segregated theta phase-coupling for cognitive performance. Curr Biol 2012;22(14):1314–8.
[76] Hoy KE, Bailey N, Michael M, Fitzgibbon B, Rogasch NC, Saeki T, et al. Enhancement of working memory and task-related oscillatory activity following intermittent theta burst stimulation in healthy controls. Cerebr Cortex 2016;26(12):4563–73.
[77] Cooper PS, Karayanidis F, McKewen M, McLellan-Hall S, Wong ASW, Skippen P, et al. Frontal theta predicts specific cognitive control-induced behavioural changes beyond general reaction time slowing. Neuroimage 2019;189:130–40.
[78] Luck SJ, Vogel EK. Visual working memory capacity: from psychophysics and neurobiology to individual differences. Trends Cognit Sci 2013;17(8):391–400.
[79] Reinhart RMG, Nguyen JA. Working memory revived in older adults by synchronizing rhythmic brain circuits. Nat Neurosci 2019;22(5):820–7.
[80] Hill AT, Rogasch NC, Fitzgerald PB, Hoy KE. Impact of concurrent task performance on transcranial direct current stimulation (tDCS)-Induced changes in cortical physiology and working memory. Cortex 2019;113:37–57.
[81] Bakulin I, Zabirova A, Lagoda D, Poydasheva A, Cherkasova A, Pavlov N, et al. Combining HF rTMS over the left DLPFC with concurrent cognitive activity for the offline modulation of working memory in healthy volunteers: a proof-of-concept study. Brain Sci 2020;10(2).